applied sciences

MDPI

Article

Taxonomic Structure Evolution, Chemical Composition and Anaerobic Digestibility of Microalgae-Bacterial Granular Sludge (M-BGS) Grown during Treatment of Digestate

Joanna Kazimierowicz [1,*], Marcin Dębowski [2] and Marcin Zieliński [2]

[1] Department of Water Supply and Sewage Systems, Faculty of Civil Engineering and Environmental Sciences, Bialystok University of Technology, 15-351 Bialystok, Poland
[2] Department of Environment Engineering, Faculty of Geoengineering, University of Warmia and Mazury in Olsztyn, 10-720 Olsztyn, Poland
* Correspondence: j.kazimierowicz@pb.edu.pl

Abstract: The liquid fraction from the dewatering of digested sewage sludge (LF-DSS) represents a major processing complication for wastewater treatment facilities, thus necessitating new and effective methods of LF-DSS neutralization. This pilot-scale study examined the evolution of a *Chlorella* sp. monoculture into microalgal-bacterial granular sludge (M-BGS) during treatment of LF-DSS in a hybrid photo-bioreactor (H-PBR). The M-BGS reached a stable taxonomic and morphological structure after 60 days of H-PBR operation. The biomass was primarily composed of *Chlorella* sp., *Microthrix parvicella*, and type 1851 and 1701 filamentous bacteria. A greater abundance of bacteria led to a faster-growing M-BGS biomass (to a level of 4800 ± 503 mgTS/dm^3), as well as improved TOC and COD removal from the LF-DSS (88.2 ± 7.2% and 84.1 ± 5.1%). The efficiency of N/P removal was comparable, since regardless of the composition and concentration of biomass, it ranged from 68.9 ± 3.1% to 71.3 ± 3.1% for N and from 54.2 ± 4.1% to 56, 2 ± 4.6% for P. As the M-BGS taxonomic structure evolved and the C/N ratio improved, so did the anaerobic digestion (AD) performance. Biogas yield from the M-BGS peaked at 531 ± 38 cm^3/gVS (methane fraction = 66.2 ± 2.7%). It was found that final effects of AD were also strongly correlated with the N and TOC content in the substrate and pH value. A mature M-BGS significantly improved settleability and separability through filtration.

Keywords: microalgal-bacterial consortia; microbial granules; microalgae-bacterial granular sludge; taxonomic evolution; digestate treatment; anaerobic digestion; biogas; methane

Citation: Kazimierowicz, J.; Dębowski, M.; Zieliński, M. Taxonomic Structure Evolution, Chemical Composition and Anaerobic Digestibility of Microalgae-Bacterial Granular Sludge (M-BGS) Grown during Treatment of Digestate. *Appl. Sci.* **2023**, *13*, 1098. https://doi.org/10.3390/app13021098

Academic Editor: Leonel Pereira

Received: 30 December 2022
Revised: 11 January 2023
Accepted: 12 January 2023
Published: 13 January 2023

1. Introduction

In light of the increasingly stringent standards regarding treated effluent, new and efficient waste treatment processes need to be identified. Research and deployment efforts target solutions that can efficiently remove organics and neutralize substances that promote microbial growth [1–3]. Environmental benefits and reduced investment/operational costs are prioritized [4]. The main deciding factors in choosing a wastewater treatment process include its compatibility with the frameworks and strategies, as well as the energy and environmental policies currently in place [5]. The deployed technologies should be in line with the principles of circular economy, zero waste policy, and energy/material recycling [6,7]. Also of importance is managing energy consumption by improving system efficiency, energy recovery, and harvesting of value-added products [8,9]. This can support environmental protection efforts aimed at promoting alternative energy sources and sustainability [10,11]. Microbial granules can serve as an alternative to conventional technologies [12]. There has been fast-growing interest in methods harnessing aerobic granular sludge (AGS) and anaerobic granular sludge (AnGS), as well as microbial-bacterial

granules (M-BGS), as evidenced by the fast-growing number of studies on the subject, and by the number commercial installations developed [13,14].

AGS and AnGS sewage treatment systems have already gone beyond the stage of research and experimental work [15,16]. Their technological readiness level is sufficient for commercial-scale design and deployment. There is, however, a new and underexplored direction in biotechnological microbial granulation—systems that harness microalgae-bacteria symbiosis [17]. Results obtained and published so far on M-BGS have earned them a reputation as a very promising and versatile new technology, which can serve as an alternative to current wastewater treatment processes [18,19]. Research on generating and successfully harnessing M-BGS is still in its early stage. So far, experiments tend to be small-scale (mostly laboratory-scale) [18–20]. The current focus is mostly on selecting optimal conditions and process parameters. However, of equal importance is the screening of the right operational data and environmental parameters for reproducible and efficient M-BGS granulation [21].

Adding microalgal biomass to the M-BGS boosts nitrogen and phosphorus removal rates compared with conventional AGS [22]. It has also been demonstrated that granules formed through microalgae-bacteria symbiosis store more fatty substances, directly adding to their calorific value [23]. This lipid content makes M-BGS biomass a more universal and valuable substrate for energy production. M-BGS can also accumulate other value-added substances, whose recovery from the surplus sludge may be technologically and commercially viable [24]. This is part of the reason why M-BGSs are emerging as a promising and sustainable method for biotechnological wastewater treatment. Commonly cited advantages of this type of biomass include: easy separation, excellent settleability, high pollutant removal rates, lower running (aeration) costs, and production of high-value-added biomass [25].

There is a dearth of semi-industrial and pilot-scale experiments that would explore M-BGS granule formation mechanisms. The majority of the studies have been conducted in laboratory scale [18–20]. Scaled-up experiments are needed to identify real-world constraints and technological/operational hurdles. The resultant findings could be used to obtain a realistic balance of investment and operating costs, as well as an assessment of environmental performance [17]. These experiments would also provide a basis and sufficient data for a life cycle assessment (LCA) [26]. So far, little focus has been devoted to exploring how taxonomic classifications and chemical profile of M-BGS affect the anaerobic digestion process and its products. This is all the more important as anaerobic digestion is the primary method for stabilizing and neutralizing wastewater treatment sludge [27,28].

The aim of the present study was to evaluate taxonomic structure evolution, chemical composition and anaerobic digestibility of microalgal-bacterial granular consortia (M-BGS) generated during treatment of liquid fraction digested sewage sludge (LF-DSS) in a hybrid, pilot-scale photo-bioreactor (H-PBR).

2. Materials and Methods

2.1. Experimental Design

The experiment was run on a semi-industrial scale in a hybrid photo-bioreactor (H-PBR) with a total volume of 2.0 m^3, fed with the liquid fraction from the dewatering of digested sewage sludge (LF-DSS). The H-PBR was sited at the "Łyna" Municipal Water Treatment Plant in Olsztyn. Parameters tested were: M-BGS biomass growth, evolution of the M-BGS taxonomic structure, changes in M-BGS chemical composition, pollutant removal by M-BGS from the medium, and applicability of M-BGS biomass as feedstock for anaerobic digestion. The experiment was divided into two stages. Stage 1 examined the growth and profile of the M-BGS biomass, as well as pollutant removal from the medium (LF-DSS). This stage (S1) was divided into five phases of H-PBR operation, according to running time (in days). The phases were demarcated based on biomass separation: phase 0—start of experiment (P0), phase 1—days 1 to 15 (P1), phase 2—days 16 to 30 (P2), phase 3—days 31 to 45 (P3), and phase 4—days 46 to 60 (P4). Stage 2 (S2) encompassed

respirometric tests on anaerobic digestion of M-BGS from the different phases of consortium maturity in S1. The experimental outline is presented in Figure 1.

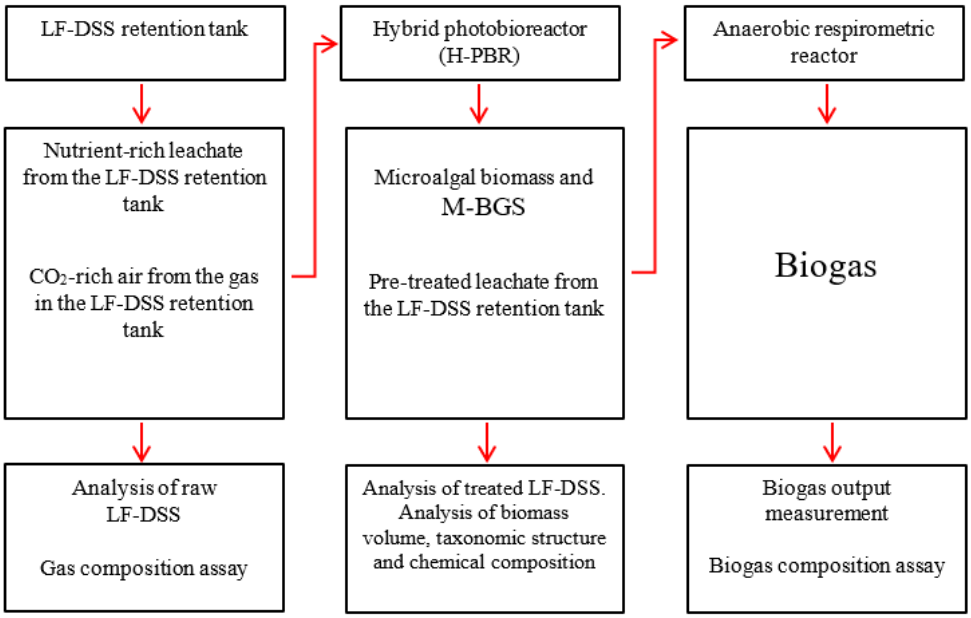

Figure 1. Flowchart of the experiment.

2.2. Location

The study was conducted at the "Łyna" Municipal Water Treatment Plant (MWWTP) in Olsztyn (GPS: 53.815152915752584, 20.453615071281686) with an average daily Q = 60,000 m^3/d. The wastewater treatment process was based on activated sludge with enhanced removal of nutrients. Wastewater was supplied from the surrounding areas by a sewer system and a fleet of gully emptiers (88 km^2, population 175,000). The untreated wastewater consisted of 80% household waste and 20% industrial effluent. Surplus sludge was stabilized by anaerobic digestion, then dewatered by chamber filter presses and sent to be managed in the environment or disposed of in an incinerator. The liquid fraction of the digestate (LF-DSS) was periodically diverted into the retention tank, from which it was recirculated to the MWWTP bioprocessing chambers. This results in periodic spikes in system load and the resultant processing difficulties, spurring researchers to explore alternative solutions for neutralizing digestate—including by harnessing microalgae biomass. The location of the experiments is shown in Figure 2.

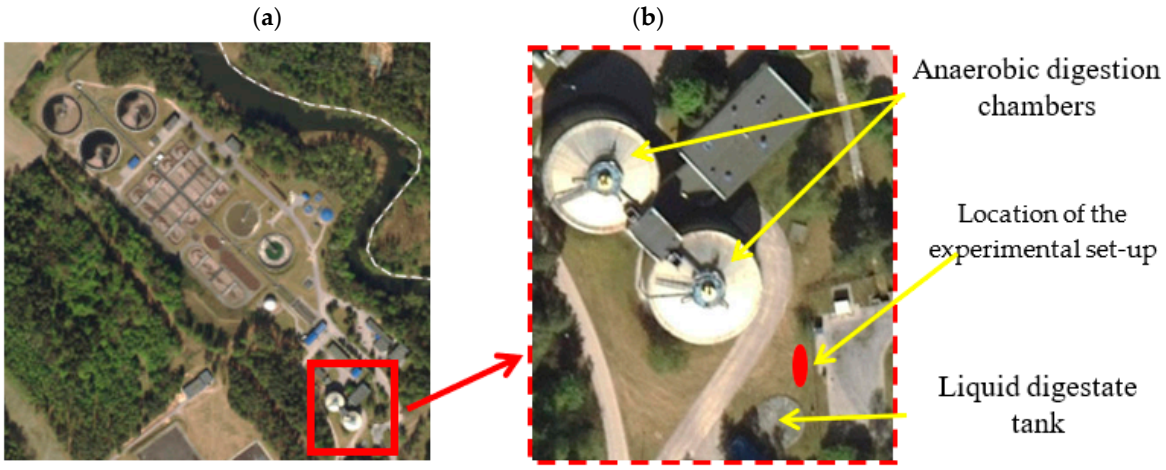

Figure 2. Location of the experiment (**a**) general view of the MWWTP "Łyna" in Olsztyn, (**b**) location of the semi-industrial H-PBR.

2.3. Materials

2.3.1. Stage 1—LF-DSS Treatment and M-BGS Production

Chlorella sp. biomass (UTEX 636) was used for the experiment. The microalgae were cultivated in and pre-adapted to the medium on leachate from anaerobic waste digesters. Initial microalgal biomass concentration in the photo-bioreactor was 500 mgTS/dm^3. The experiment proper was commenced after one full hydraulic residence period in the H-PBR.

Liquid fraction of digested sewage sludge (LF-DSS)—sourced from the MWWTP in Olsztyn and collected in a retention tank—was used as the medium for treatment and for growing microalgae into microalgal-bacterial granular consortia, then into M-BGS. The digested sewage sludge was sourced from a digester running under the following operating parameters: organic load rate (OLR)—approx. 2.0 kg DOM/m^3·d, hydraulic retention time (HRT)—20 days, process temperature—35 °C. The liquor from DSS dewatering by chamber filter presses was stored in a 1000 m^3 underground retention tank, then fed into the H-PBR. The H-PBR, with an active volume of 1.0 m^3, was supplied with 100.0 dm^3 LF-DSS/d. Hydraulic retention time (HRT) was 10 days. At the start of the experiment, the H-PBR was fed with 50% treated effluent and 50% LF-DSS. The digesters and the LF-DSS storage tank are shown in Figure 3.

Figure 3. LF-DSS storage tank (**a**), enclosed digester and chamber filter press building, with the H-PBR in the foreground (**b**).

Carbon dioxide and oxygen were supplied to the H-PBR microbial community in the form of diffused ambient air and CO_2-rich air from the gas in the LF-DSS tank. The air was bubbled in through the bottom of the H-PBR at 50 m^3/h. The profiles of the LF-DSS and the air from the gas phase of the LF-DSS storage tank are given in Table 1.

Table 1. Composition of the LF-DSS and air fed into the PBR.

LF-DSS		
Indicator	**Unit**	**Value**
COD	mgO_2/dm^3	719.3 ± 57
TOC	mgC/dm^3	524 ± 62
TP	mgP/dm^3	26.8 ± 1.8
P-PO_4	mg P-PO_4/dm^3	21.1 ± 2.4
TN	mgN/dm^3	52.9 ± 4.7
N-NH_4	mg N-NH_4/dm^3	46.3 ± 3.9
pH	-	7.24 ± 0.13

Table 1. *Cont.*

LF-DSS		
Indicator	**Unit**	**Value**
	Air	
Indicator	Unit	Value
CO_2	ppm	790 ± 70
H_2S	ppm	120 ± 30
O_2	%	20.81 ± 0.12
N_2	%	77.94 ± 0.11

2.3.2. Stage 2—M-BGS Anaerobic Digestion

The anaerobic respirometers were inoculated with anaerobic sludge (AS) sourced from continuous-flow anaerobic digesters (which processed a biomass of 70% *Chlorella* sp. *w/w*. and 30% *Scenedesmus* sp. *w/w*) [29]. The inoculum was sourced from fully-stirred digesters. The temperature in the reactors was kept constant at 38 °C. Initial concentration of anaerobic sludge was approx. 4.0 gTS/dm^3. Organic load rate (OLR) was kept at 2.0 gVS/dm^3·d. Hydraulic retention time (HRT) was 40 d. The feedstock supply was halted for 10 days before the anaerobic sludge was injected into the respirometric reactors. The inoculum profile is given in Table 2.

Table 2. Profile of the digester inoculum (anaerobic sludge).

Indicator	**Unit**	**Value**
TS	% FM	4.7 ± 1.3
VS	% TS	70.9 ± 2.5
TN	mg/gTS	45.3 ± 3.1
TP	mg/gTS	4.0 ± 1.0
TC	mg/gTS	384 ± 29
TOC	mg/gTS	316 ± 30
C:N	-	6.9 ± 0.2
pH	-	6.7 ± 0.2
protein	% TS	28.3 ± 1.9
lipids	% TS	6.1 ± 0.8
saccharides	% TS	1.8 ± 0.5

2.4. Experimental Set-Up

2.4.1. Stage 1—LF-DSS Treatment and M-BGS Production

The experiment was conducted in a hybrid closed raceway photo-bioreactor (H-PBR) of our own design. The active volume of the H-PBR was 1.0 m^3 with a depth of 0.3 m. A single four-blade mechanical agitator was fitted to the longer straight side of the reactor. The agitator ran at 30 rpm for a circulation flow rate of 0.5 m/s. To provide adequate illumination during low-sunlight periods, tri-band fluorescent lamps with narrowband phosphors were used, providing 100 lumens of white light per one watt of energy consumed. The lighting array (fluorescent lamps) was distributed along the central axis of the reactor over approx. 0.6 m^2. The H-PBR was capped with a transparent, sunlight-permeable covers. The sunlight-permeable reactor surface (transparent covers) was approx. 2.6 m^2. The heating was provided by electrical heaters with a heating capacity of 1.0 kW. The heating activated automatically when the medium temperature was at 20 °C, and deactivated at 22 °C. The sides and bottom of the H-PBR were thermally insulated with an approx. 0.15 m

layer of polystyrene foam. To provide thermal protection, the transparent cover consisted of two layers with an air pocket in-between. The H-PBR was fitted with valves for metering the LF-DSS, valves for supplying air from the LF-DSS storage tank, drains, and a central partition for providing circular flow. The microalgae biomass was thickened and removed from the system using a two-stage drum microsieve array with 10.0 µm (1st filtration pass) and 5.0 µm (2nd filtration pass) meshes, as well as a sedimentation step. The pre-treated leachate was recirculated into the PBR and reused for the next phase of the experiment. The individual components of the experimental set-up are shown in Figure 4.

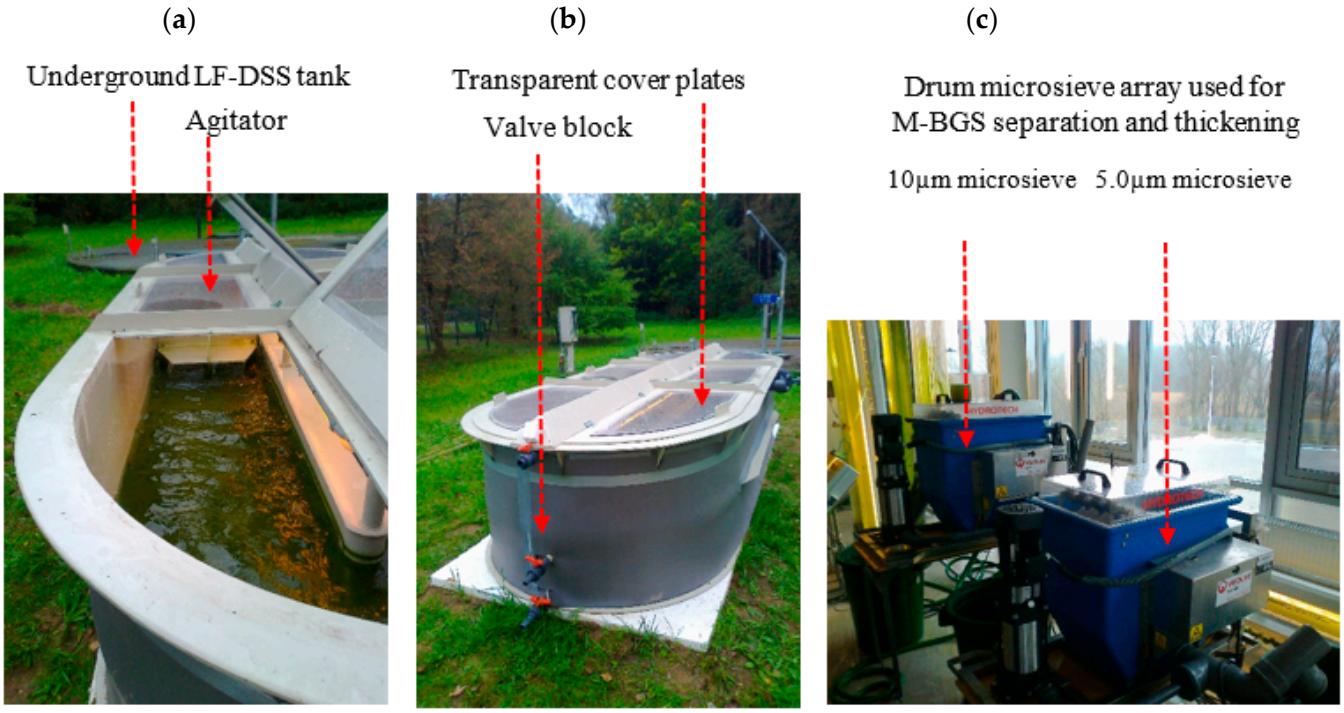

Figure 4. Experimental set-up for LF-DSS treatment (**a**,**b**) coupled with M-BGS production and a two-stage biomass separation system (**c**).

2.4.2. Stage 2—M-BGS Anaerobic Digestion

The performance of the M-BGS anaerobic digestion was assessed using the volumetric gas production method in batch respirometric reactors (AMPTS II, BPC Instruments AB, Lund, Sweden). The digestion process was run at 38 ± 1 °C. The bioreactors were equipped with a vertical agitator, which ran for 30 s every 10 min at 100 rpm. The active volume of the respirometers was 500 cm^3. Initial organic load rate (OLR) was 5.0 gVS/dm^3. To ensure anaerobic conditions in the respirometers prior to the measurements, the system was purged with 150 dm^3/h pure nitrogen for 5 min. Digestion continued for 40 d. Biogas composition was monitored chromatographically. The measurement system was equipped with an ex-situ CO_2 adsorption unit, fixing the CO_2 from the biogas with 3M NaOH. A biomethane output report was logged once a day using a program that generates results for a normalized gas volume (standard atmospheric pressure of 101.3 kPa at 0 °C and zero humidity). Endogenous biogas generated by anaerobic sludge was excluded from the calculation. A diagram of the experimental equipment is presented in Figure 5.

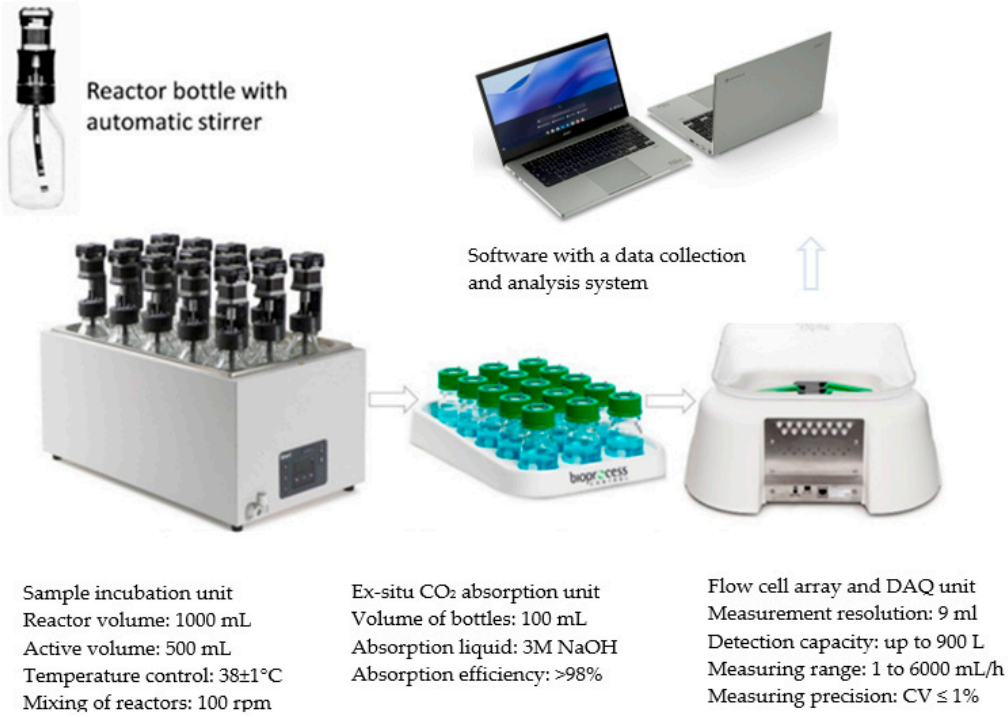

Figure 5. Diagram of the experimental set-up used in stage 2 of the study.

2.5. Analytical Methods

TS and vs. were determined gravimetrically at 105 °C. TN, N-NH_4, TP, P-PO_4 and COD were quantified using Hach Lange cuvette tests and a UV/VIS DR 5000 spectrophotometer with a HT 200 s mineralizer (Hach-Lange GmbH, Düsseldorf, Germany). The TOC content was determined by means of a TOC-L analyzer (Shimadzu, Kyoto, Japan). Lipids were quantified using the Soxhlet method with a Buchi extraction apparatus (Flawil, Switzerland). Biomass samples dried at 105 °C were analyzed for the contents of total carbon (TC), total organic carbon (TOC), and total nitrogen (N_{total}) (Flash 2000 analyzer, Thermo Scientific, Waltham, MA, USA). Total protein was calculated by multiplying the value of N_{total} by the protein conversion factor of 6.25. Total phosphorus (P_{tot}) was quantified colorimetrically with ammonium metavanadate (V) and ammonium molybdate, after prior sample mineralization in a mixture of sulfuric (VI) and chloric (VII) acids with a DR 2800 spectrophotometer (Hach-Lange GmbH, Düsseldorf, Germany) at a wavelength of 390 nm. The pH value of H_2O was measured potentiometrically. Reducing sugars were determined colorimetrically with an anthrone reagent at 600 nm using a HACH Lange DR 2800 spectrophotometer (Hach-Lange GmbH, Düsseldorf, Germany). Biomass sedimentability was determined by examination in measuring cylinders. Biogas composition was assayed with a GC Agillent 7890 A gas chromatograph (Agilent, Santa Clara, CA, USA). Quality of the PBR input air was determined using a GMF 430 analyzer (Gas Data, Coventry, UK). The respirometric tests were also used to determine biogas production rate (r) for each experimental variant. The reaction rate constant (k) was calculated from the experimental data by non-linear regression using Statistica 13.1 PL.

2.6. Taxonomic Identification

Taxonomic classification of microalgae was performed on non-permanent and semi-permanent slides. Qualitative and quantitative analysis of the biomass was done at microscopic magnification levels: 1.25 × 10 × 40 or 1.25 × 10 × 100. Qualitative analysis of the microalgal biomass was conducted using a Moldaenke BBE Alage OnLine Analyser. Bacteria species' structure and volume were determined in vivo. Protozoa identifiable without staining were identified at the species level, and other microbes were identified at the genus level or higher. The abundance of small flagellates was estimated in a Fuchs-Rosenthal

chamber (diagonal) along the count ranges of: <10, 10–100, >100. The abundance of large threadworms, Rhizopoda, ciliates and Eumetazoa was determined in 0.1 mL microscope slides and translated to 1 mg dry mass. Filamentous microbes were identified in vivo and in Gram- and Neisser-stained slides by S-test and PHB test. Shares of individual taxonomic groups in the biomass were estimated by the cell volume measurement method [30]. Microbes were identified in each sample separately in ten replications. Biomass was calculated by multiplying the counts by average volumes of each taxon and specific mass (1.0 g·cm^{-3}).

2.7. Statistical Methods

The experiment was carried out in triplicate. Statistical analysis was performed using Statistica 13.1 PL. Tukey's (HSD) test and ANOVA were applied to determine significant differences between the variables. Differences were considered significant at $p = 0.05$.

3. Results and Discussion

3.1. Stage 1—LF-DSS Treatment and M-BGS Production

3.1.1. Biomass Growth

For the first two cycles of H-PBR operation, the biomass grew along the typical pattern for microalgae. The initial 3 days marked the adaptation (lag) phase, (Figure 6a). During this time, microalgae concentration grew from 500± mgTS/dm^3 to 760 ± 83 mgTS/dm^3. The biomass then proceeded to grow exponentially until day 12, when it reached 3050 ± 94 mgTS/dm^3. Days 13 to 15 were when the growth rate decelerated and reached the stationary phase, with the final biomass concentration being 3210 ± 140 mgTS/dm^3 (Figure 6a). The growth rate throughout the exponential phase was 268 ± 12 mgTS/dm^3·d. At the outset of the second cycle (days 16 to 30), the lag phase lasted 3 days, just as before. The growth rate for the nascent M-BGS ranged from 610 ± 139 mgTS/dm^3 to 930 ± 77 mgTS/dm^3, only to accelerate in the subsequent days (Figure 6b). Exponential growth was maintained for the next 8 days, reaching 3260 ± 199 mgTS/dm^3 by day 26. The microbial growth rate then leveled off, reaching the stationary phase at 3610 ± 242 mgTS/dm^3 (Figure 6b). During the exponential phase, the growth rate was significantly higher than before, reaching 296 ± 17 mgTS/dm^3·d.

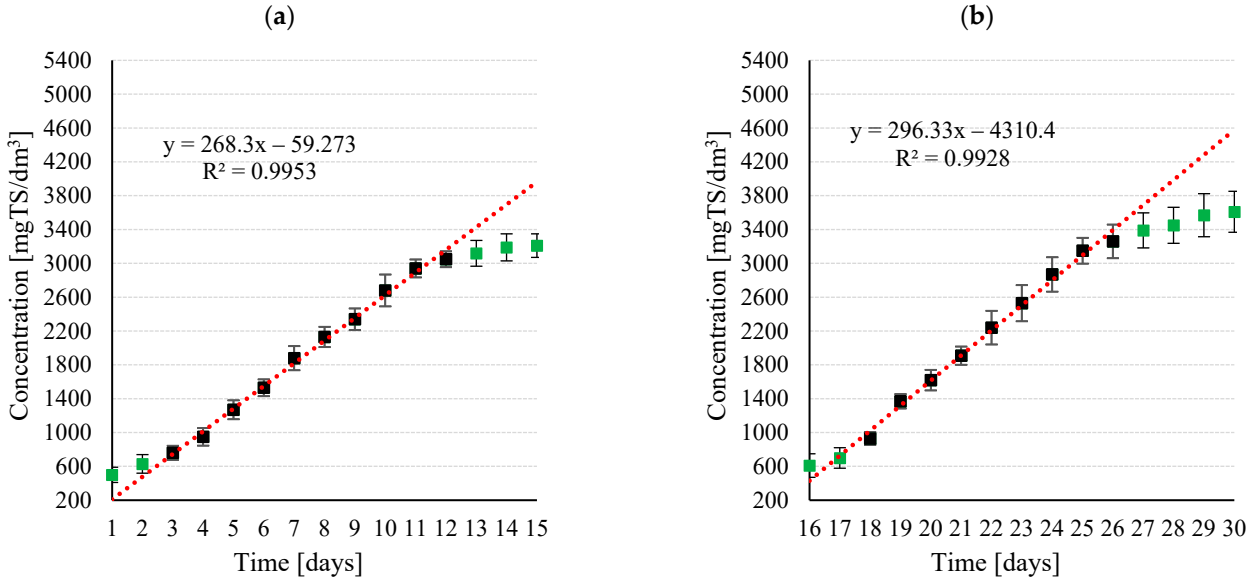

Figure 6. M-BGS biomass production in phases: (**a**) phase 1 (days 1–15) and (**b**) phase 2 (days 16–30) of the H-PBR operation.

M-BGS growth was significantly higher in the next experimental cycle. The large abundance of bacteria caused the growth curve to diverge from the normal pattern for

microalgae, as the microbial population grew at an exponential rate from the very beginning (Figure 7).

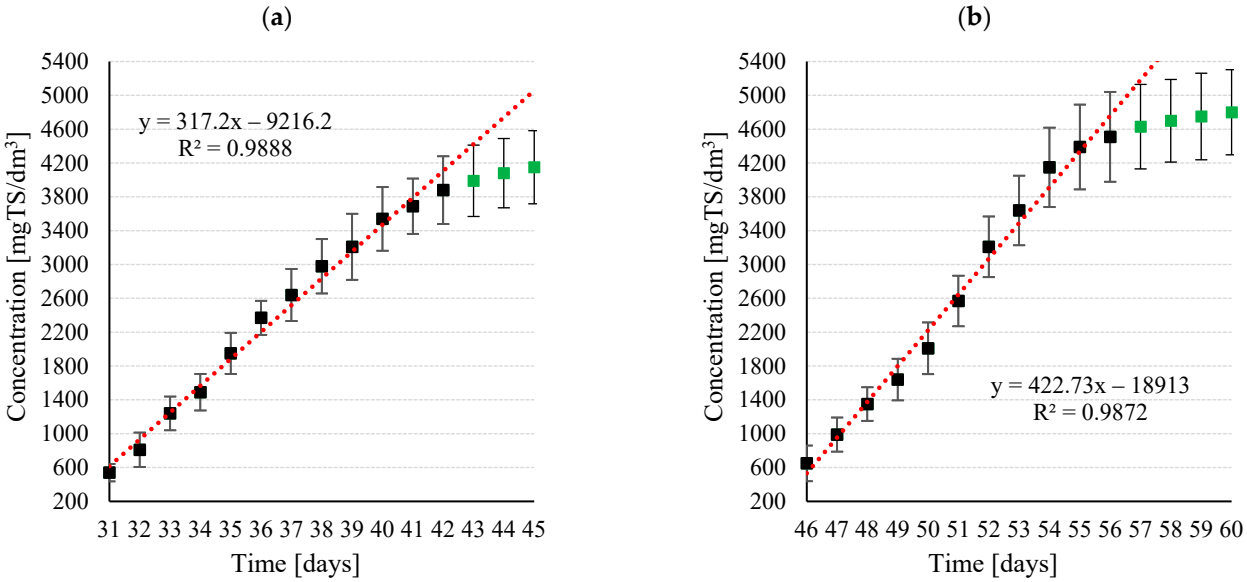

Figure 7. M-BGS biomass production in phases: (**a**) phase 3 (days 31–45) and (**b**) phase 4 (days 46–60) of the H-PBR operation.

Through days 31 to 43, the microalgae + AS microbes biomass grew from 540 ± 103 mgTS/dm^3 to 3990 ± 422 mgTS/dm^3, which translates to a growth rate of 317 ± 29 mgTS/dm^3·d. The growth rate subsequently tapered off, with no further significant increases. The final concentration at the end of the phase was 4250 ± 432 mgTS/dm^3 (Figure 7a). Throughout days 46 to 60, the microbial community entered its final stage of structure and population, and saw no further changes over the remaining period of operation. The mature M-BGS biomass grew at its highest rate—423 ± 39 mgTS/dm^3·d. No lag phase was observed. In the end, the population grew to a concentration of 4800 ± 503 mgTS/dm^3, significantly higher than in previous phases (Figure 7b).

The available literature lacks reports from studies into the use of real wastewater. It is certainly a gap that needs to be filled. More extensive research is available regarding laboratory analyses of synthetic wastewater [17]. However, it needs to be emphasized that such results require large-scale validation during the treatment of real wastewater and leachate. A study conducted by Zhang et al. (2020) [31] demonstrated that the M-BGS population grew exponentially during the treatment of synthetic domestic wastewater, leading to the ultimate biomass concentration in reactors at 5.77 ± 0.08 gTS/dm^3 [31]. In the work by Wang et al. (2021) [32], the authors proved that the biomass of microalgal-bacterial consortia might reach the concentration of 7.89 ± 0.03 gTS/dm^3 during synthetic wastewater treatment. In turn, Dong et al. (2021) [33] achieved M-BGS concentration at 4.42 ± 0.16 gTS/dm^3 in days 1 to 21 as well as 4.34 ± 0.09 gTS/dm^3 in days 22 to 23 of synthetic saline wastewater treatment. Subsequent days of the treatment process brought successive decrease in biomass concentration in the reactor, i.e., to 3.20 ± 0.11 gTS/dm^3 in days from 33 to 60 and to 1.23 ± 0.08 gTS/dm^3 in days from 61 to 110. It is generally believed that the growth of certain microorganisms in M-BGS may be severely inhibited when microbial cell structure is damaged upon the influence of high salinity conditions (like 3% in the study by Dong et al. (2021) [33]), which probably leads to the leaching of a part of M-BGS biomass from the reactor [34].

3.1.2. Taxonomic Structure

The microbial community consisted almost exclusively of *Chlorella* sp. microalgae (almost 100%TS) at PBR start-up (Figure 8). Until day 30, activated sludge microbes in total

biomass stayed within levels below 30%TS—specifically 22 ± 7%TS after 15 days of PBR operation and 29 ± 9%TS after 30 days (Figure 9).

(**a**) (**b**)

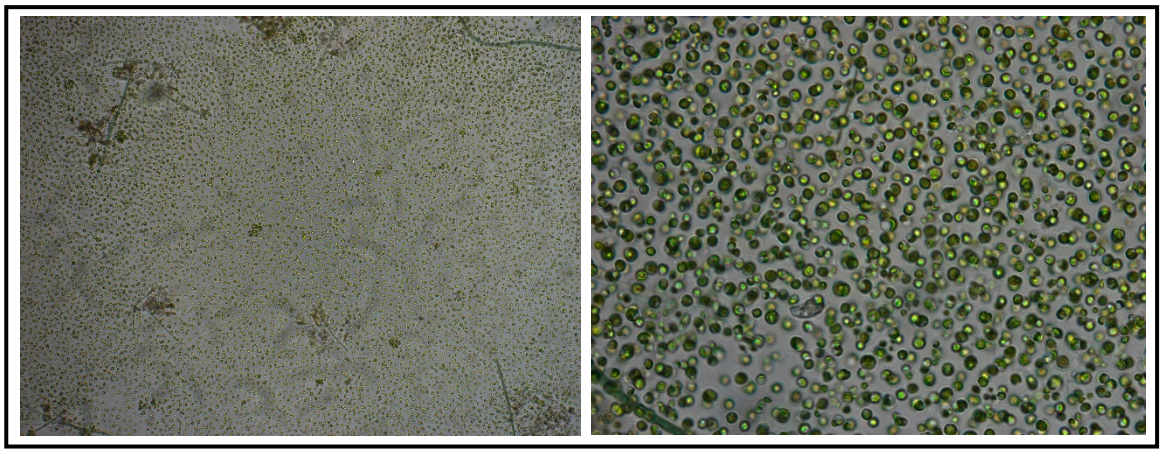

Figure 8. *Chlorella* sp. biomass at the beginning of the experimental cycle with microscopic magnification (**a**) ×10, (**b**) ×100.

(**a**) (**b**)

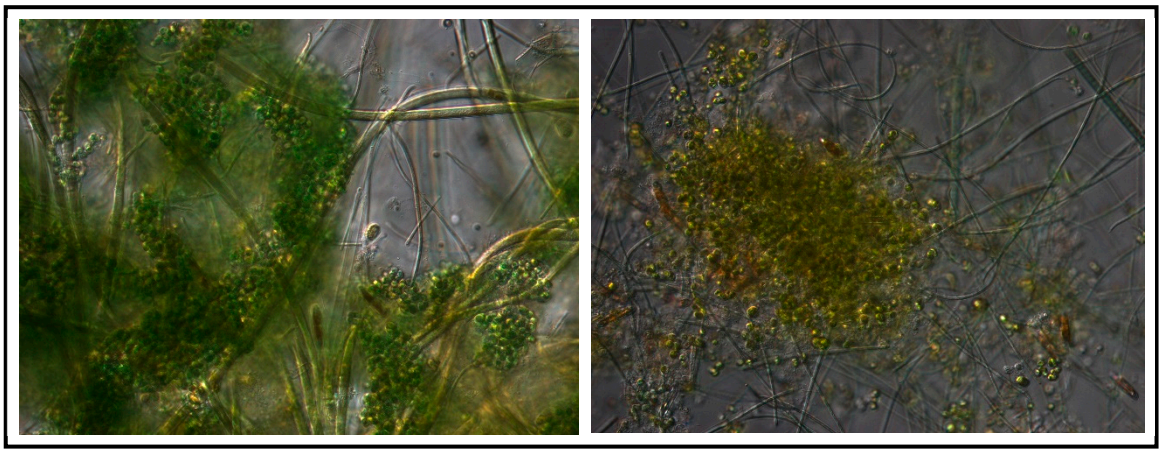

Figure 9. Characteristic views with microscopic magnification ×100 of microalgal-bacterial consortia produced after (**a**) 15 and (**b**) 30 days of H-PBR operation.

The share of bacteria and protozoa in the evolving M-BGS was identified after 45 days of experiment. Heterotrophic microbes accounted for 47 ± 12%TS (Figure 10). After 60 days, activated sludge microbes accounted for approx. 43 ± 9%TS of the entire M-BGS community. The taxonomic structure was stable throughout the remainder of H-PBR operation (Figure 11).

The artificial ecosystem that emerged in the LF-DSS was abundant not only in *Chlorella* sp. microalgae, but also in filamentous *Microthrix parvicella*, type 1851 and 1701 filamentous bacteria, and *Streptococcus* sp. Unicellular species were much slower to grow and represented a minor fraction of the M-BGS community. *Pseudomonas* sp., *Nitrosomonas* sp., *Azotobacter* sp., *Achromobacter* sp., *Flavobacterium* sp., *Micrococcus* sp., *Staphylococcus* sp., *Bacillus* sp., and *Mycobacterium* sp. bacteria were detected. Protozoa were mainly represented by ciliates, *Aspidisca cicada*, *Drepanomonas revoluta* and *Vorticella infusionum*. On average, their shares in the total protozoa population were 61, 15 and 6%, respectively. Also found were sapropelic flagellates *Trigonomonas*, *Paramecium caudatum*, and unsupported Rhizopoda.

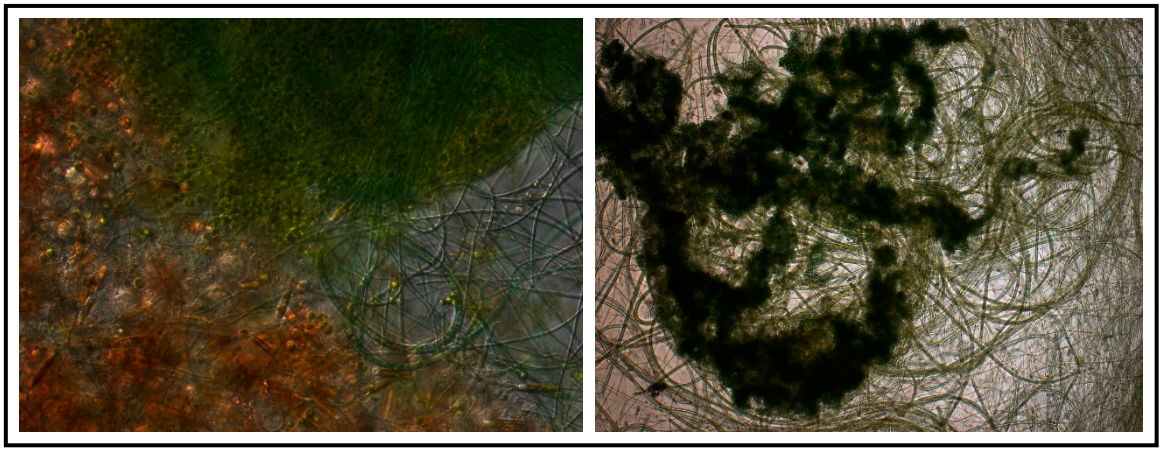

Figure 10. Characteristic views with microscopic magnification ×100 of the evolving M-BGS after 45 days of H-PBR.

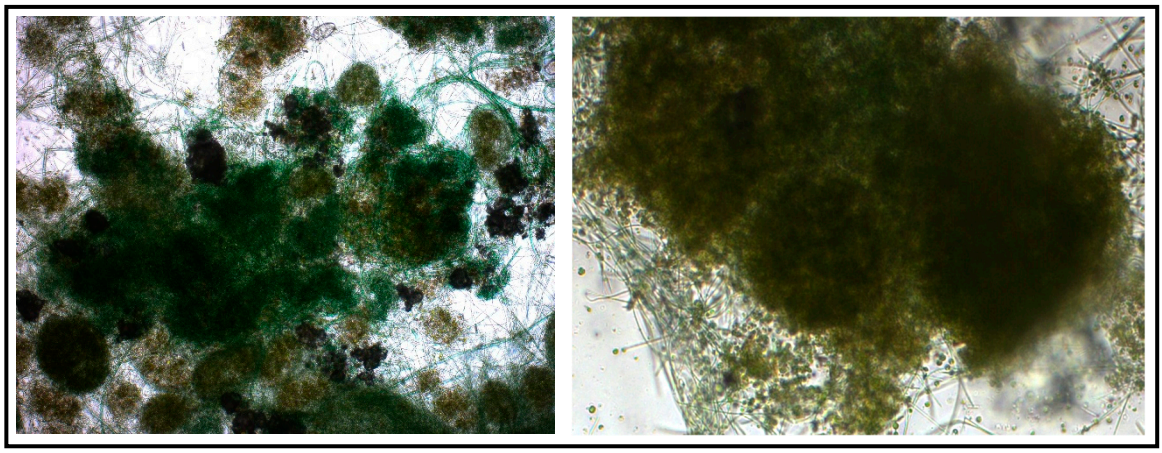

Figure 11. Characteristic views with microscopic magnification ×100 of M-BGS after 60 days of H-PBR operation.

Thus far, research works have demonstrated the self-aggregation of microorganisms in photo-bioreactors to be the major mechanism of M-BGS formation [35]. It has been proved that granules formed in this way feature high stability, content and density, which allows for effective pollutant removal and separation of M-BGS biomass during gravitational sedimentation or simple filtration [36]. It has also been found that the presence of filamentous bacteria in the bacterial biocenosis of activated sludge is an important element in the formation of stable and compact granules. They constitute a backbone and a construction of a granule, to which further cells of bacteria and microalgae are attached by means of exogenous polymeric substances [37]. In the study by Shen et al. (2021) [38], the major functional groups classified at the genus level in the taxonomic structure of M-BGS included: *Pseudomonas*, *Thauera*, *Acinetobacter*, *Flavihumibacter*, *Pseudoxanthomonas*, *Aquimonas*, *Gemmatimonas*, and *Leptolyngbyales* [38]. As reported by Fan et al. (2021) [39], the prevailing communities of M-BGS at the genus level were *Rhizobium* and *Proteiniclasticum*. The community of eucaryotic algae was dominated by the genus *Chlorella* belonging to the class Chlorophyta [39]. It needs to be emphasized, however, that the cited authors analyzed synthetic municipal wastewater.

3.1.3. Chemical Composition of M-BGS Biomass

The lowest levels of organic substances (expressed as vs. and TOC) were found in the initial, pure *Chorella* sp. culture, at 87.9 ± 1.3% TS and 439 ± 30 mg/gTS, respectively (Table 3). As the abundance of activated sludge microbes increased in the evolving M-BGS,

the percentage of organics in TS significantly decreased. The lowest vs. levels were recorded for the 45th day of H-PBR operation onwards. The 45-day-old and 60-day-old biomass contained 80.3 ± 4.2% TS and 82.3 ± 3.5% TS, respectively, as well as 438.2 ± 81 mg/gTS and 455.0 ± 74 mg/gTS TOC, respectively (Table 3). The formation and maturation of M-BGS improved the C/N ratio—an important parameter for anaerobic digestion. At the beginning of the experimental cycle, the C/N of the microalgal biomass was 11.0 ± 1.4, which is at the lower end of the optimum range for AD (Table 3). After the first (15-day) phase of operation, the C/N was around 12.8 ± 1.3 and it steadily increased as the PBR continued running. The C/N ratio peaked at 15.6 ± 2.4 45 days into the cultivation process (Table 3). As the bacteria and protozoa proliferated in the evolving M-BGS, there was a significant reduction in protein in the biomass—from 24.9 ± 1.5%TS at start-up to 17.1 ± 2.2%TS after 45 days of cultivation. Lipid levels, on the other hand, were mostly unaffected. The microalgal biomass profiles across the PBR operation phases are given in Table 3.

Table 3. Profiles of the evolving M-BGS biomass across H-PBR operation phases.

Parameter	Unit	Value				
		Start	d 15	d 30	d 45	d 60
VS	% TS	87.9 ± 1.3	85.0 ± 2.2	84.0 ± 2.7	80.3 ± 4.2	82.3 ± 3.5
TN	mg/gTS	39.8 ± 2.4	35.0 ± 1.7	33.5 ± 3.1	27.4 ± 3.9	30.6 ± 3.4
TP	mg/gTS	16.4 ± 1.1	14.8 ± 1.8	14.3 ± 2.0	12.1 ± 3.1	13.3 ± 2.9
TC	mg/gTS	502 ± 42	477.4 ± 56	469.5 ± 72	438.2 ± 81	455.0 ± 74
TOC	mg/gTS	439 ± 30	417.2 ± 61	410.3 ± 66	382.6 ± 65	397.4 ± 70
C:N	-	11.0 ± 1.4	12.8 ± 1.3	13.3 ± 1.8	15.6 ± 2.4	14.4 ± 2.0
pH	-	7.61 ± 0.08	7.71 ± 0.09	7.52 ± 0.11	7.42 ± 0.09	7.53 ± 0.07
protein	% TS	24.9 ± 1.5	21.9 ± 2.2	20.9 ± 1.9	17.1 ± 2.2	19.1 ± 2.1
lipids	% TS	13.2 ± 0.9	12.1 ± 1.1	11.7 ± 1.0	10.3 ± 0.9	11.1 ± 1.3

Thickening and separation are some of the most difficult and costly processing steps in scaled-up microalgae cultivation. Unlike activated sludge, microalgae do not settle, and thus usually require targeted coagulation, filtration, flotation, centrifugation and other thickening steps. The symbiotically grown M-BGS significantly boosted biomass congealability. The M-BGS had very good settleability, forming dense and heavy aggregates. This structure made it easy to separate the M-BGS from the medium by means of simple drum filtration and sedimentation. The products of the two-step microfiltration and sedimentation are shown in Figure 12 and Table 4. At 60 days into the experiment (last phase), the M-BGS concentration in the PBR was 4.8 ± 0.50 gTS/dm^3. The 61 ± 4 dm^3 biomass remained after the 1st filtration pass (10.0 µm sieve) contained 59 ± 3.1 gTS/dm^3, for a total of 3600 ± 200 gTS. 939 ± 4 dm^3 of the medium was passed through the 2nd drum filtration (5.0 µm), containing 1.3 ± 0.2 gTS/dm^3 M-BGS. After the 2nd filtration pass, 84 ± 2 dm^3 biomass was thickened to a concentration of 14 ± 1.3 gTS/dm^3, for a total M-BGS mass of 1175 ± 110 gTS/dm^3. The final effluent contained 0.029 ± 0.01 gTS/dm^3 (Table 4).

Table 4. Products of algal biomass filtration.

Parameter	Unit	Reactor	1st-Pass Filtrate	1st-Pass Effluent	2nd-Pass Filtrate	2nd-Pass Effluent
Volume	dm^3	1000	61 ± 4	939 ± 4	84 ± 2	855 ± 2
Biomass concentration	gTS/dm^3	4.8 ± 0.5	59 ± 3.1	1.3 ± 0.2	14 ± 1.3	0.029 ± 0.01
Biomass quantity	gTS	4800 ± 503	3600 ± 200	1200 ± 190	1175 ± 110	25 ± 0.8
Water content	%	99.52 ± 0.31	94.10 ± 0.24	99.76 ± 0.12	98.60 ± 0.22	99.98 ± 0.01

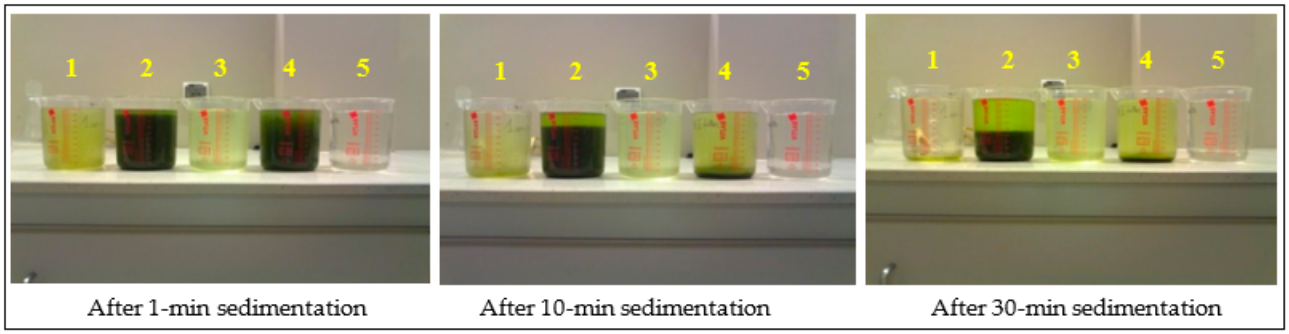

Figure 12. Products of M-BGS separation via 2-stage filtration and sedimentation (1—H-PBR growth medium, 2—M-BGS after 1st filtration pass, 3—effluent after 1st filtration pass, 4—biomass after 2nd filtration pass, 5—effluent after 2nd filtration pass).

3.1.4. Pollutant Removal Rate

The changes in the M-BGS proved to have a significant effect on organic matter removal from the LF-DSS. We found that the more bacteria and protozoa were in the biomass, the better the biodegradation of waste substances (COD and TOC) was. In phase 1 (P1) of H-PBR (*Chlorella* sp.-dominated microbial community), COD and TOC removal was 61.4 ± 2.3%, and 71.9 ± 2.7%, respectively (Table 5). Nominal levels in the effluent were 277 ± 22 mgO_2/dm^3 and 147 ± 17 mg/dm^3, respectively. P2 (days 16–30) and P3 (days 31–45) had similar organic biodegradation rates, which were, respectively, 73.1 ± 1.7% and 75.8 ± 3.2% for COD and 80.7 ± 3.0% and 83.4 ± 4.7% for TOC. COD in the effluent did not exceed 100 mgO_2/dm^3, whereas TOC did not exceed 200 mg/dm^3—significantly less than in P1 (Table 5). P4 (days 46 to 60 of H-PBR operation) performed the best in terms of organics removal—the COD in the treated LF-DSS was 114 ± 9 mgO_2/dm^3, meaning that 84.1 ± 5.1% was biodegraded. TOC removal was 88.2 ± 7.2%, leaving 61.8 ± 7.4 mg/dm^3 in the effluent (Table 5).

Table 5. Indicators of LF-DSS treatment performance.

Parameter	Final Concentration (mg/dm^3)				Removal (%)			
	d 15	d 30	d 45	d 60	d 15	d 30	d 45	d 60
COD	277 ± 22	193 ± 15	174 ± 14	114 ± 9	61.4 ± 2.3	73.1 ± 1.7	75.8 ± 3.2	84.1 ± 5.1
TOC	147 ± 17	99.0 ± 12	87.0 ± 10.3	61.8 ± 7.4	71.9 ± 2.7	80.7 ± 3.0	83.4 ± 4.7	88.2 ± 7.2
TP	7.69 ± 0.82	7.54 ± 0.81	7.58 ± 0.81	7.36 ± 0.79	54.2 ± 4.1	55.1 ± 3.9	54.9 ± 3.8	56.2 ± 4.6
$P\text{-}PO_4$	0.98 ± 0.23	1.25 ± 0.30	1.19 ± 0.28	1.10 ± 0.26	90.3 ± 1.7	87.6 ± 1.2	88.2 ± 2.3	89.1 ± 1.1
TN	15.2 ± 1.3	15.6 ± 1.4	17.4 ± 1.6	16.5 ± 1.5	71.3 ± 3.1	70.5 ± 2.9	67.2 ± 2.4	68.9 ± 3.1
$N\text{-}NH_4$	5.00 ± 0.42	4.31 ± 0.36	5.93 ± 0.50	5.51 ± 0.46	89.2 ± 1.4	90.7 ± 1.7	87.2 ± 1.3	88.1 ± 1.6
Parameter	**Load in**				**Load removed**			
	d 15	d 30	d 45	d 60	d 15	d 30	d 45	d 60
COD	71.9 ± 5.7				44.1 ± 3.5	52.6 ± 4.2	54.5 ± 4.3	60.5 ± 4.8
TOC	52.4 ± 6.2				37.7 ± 4.4	42.3 ± 5.0	43.7 ± 5.2	46.2 ± 5.5
TP	2.68 ± 0.18				1.45 ± 0.14	1.48 ± 0.11	1.47 ± 0.09	1.51 ± 0.16
$P\text{-}PO_4$	2.11 ± 0.24				1.91 ± 0.22	1.85 ± 0.20	1.86 ± 0.18	1.88 ± 0.32
TN	5.29 ± 0.47				3.77 ± 0.33	3.73 ± 0.45	3.55 ± 0.24	3.64 ± 0.32
$N\text{-}NH_4$	4.63 ± 0.39				4.13 ± 0.47	4.20 ± 0.71	4.04 ± 0.62	4.08 ± 0.91
Parameter	**Biomass gained [gTS/g_{in}]**				**Biomass gained [TS/g_{rem}]**			
	d 15	d 30	d 45	d 60	d 15	d 30	d 45	d 60
COD	3.73 ± 0.39	6.70 ± 0.51	6.03 ± 0.72	7.74 ± 0.93	6.07 ± 0.22	5.63 ± 0.47	5.82 ± 0.64	6.98 ± 0.88
TOC	5.11 ± 0.68	5.65 ± 0.43	6.05 ± 0.88	8.05 ± 1.02	7.11 ± 0.83	7.00 ± 0.63	7.25 ± 1.01	9.13 ± 1.14
TP	100 ± 12	110 ± 11	118 ± 14	157 ± 17	184 ± 19	200 ± 23	215 ± 18	280 ± 22
$P\text{-}PO_4$	127 ± 16.1	140 ± 12.9	150 ± 17.3	200 ± 21.5	141 ± 18.9	160 ± 14.6	170 ± 17.9	224 ± 23.8
TN	50.7 ± 5.2	56.0 ± 3.1	59.9 ± 5.4	79.8 ± 5.9	71.1 ± 6.3	79.4 ± 4.8	89.2 ± 9.1	115.8 ± 11.0
$N\text{-}NH_4$	57.9 ± 5.9	63.9 ± 4.0	68.5 ± 5.8	91.1 ± 8.1	64.9 ± 7.2	70.5 ± 5.5	78.5 ± 6.1	103 ± 9.9

The different rates of organics biodegradation produced significant variance in the loads removed during LF-DSS treatment. COD removal ranged from 44.1 ± 3.5 gCOD/d in P1 to 60.5 ± 4.8 gCOD/d in P4. The rates for TOC ranged from 37.7 ± 4.4 gCOD/d in P1 to 46.2 ± 5.5 gCOD/d in P4 (Table 5). The biomass levels in the H-PBR (Figure 13) and the proportion of heterotrophic microbes in the M-BGS were found to correlate with organic removal rates and final organic levels (Figure 14).

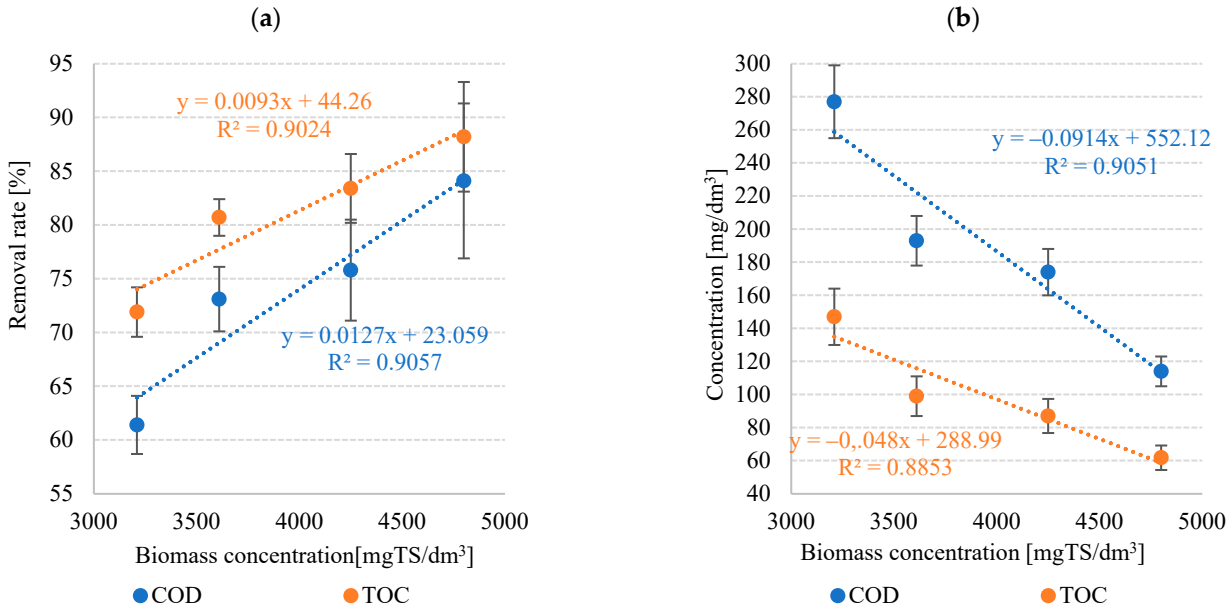

Figure 13. Correlations between M-BGS levels and (**a**) organics removal and (**b**) levels of organic matter in the H-PBR effluent.

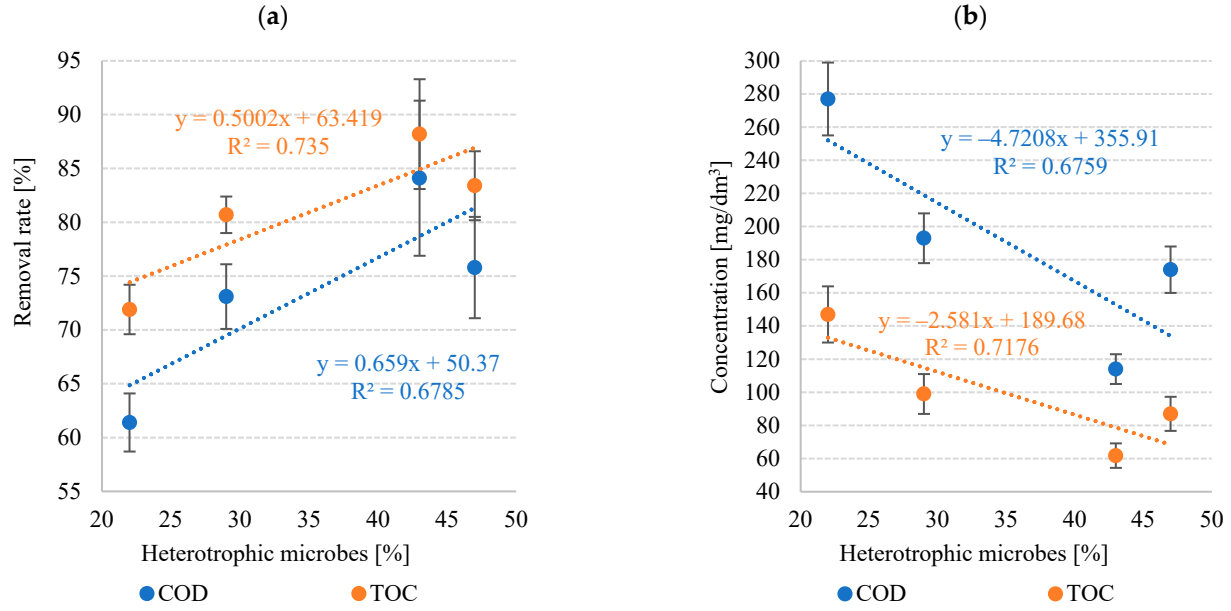

Figure 14. Correlations between the abundance of activated sludge microbes in the M-BGS and (**a**) organics removal and (**b**) levels of organic matter in the PBR effluent.

The results indicate that changes in the taxonomic structure of the biomass did not significantly affect N and P removal from the LF-DSS. Final performance was similar across all phases of the experiment (Table 5). TN removal ranged from 67.2 ± 2.4% in F3 to in F1, meaning that the final levels in the effluent were 15.2 ± 1.3 mgN/dm^3 to 17.4 ± 1.6 mgN/dm^3. The differences were not statically significant. Treatment perfor-

mance for P was similar across all PBR operation phases. TP in the final effluent fell within the narrow range of 7.36 ± 0.79 mgP/dm^3 to 7.69 ± 0.82 mgP/dm^3, whereas P-PO_4 ranged from 0.98 ± 0.23 mg/dm^3 to 1.25 ± 0.30 mg/dm^3. Indicators of LF-DSS treatment performance (pollutant removal rate, levels in effluent, load removed and specific M-BGS biomass growth) are given in Table 5.

It is claimed that in the symbiotic growth systems of M-BGS structures, microalgae are responsible for the intensification of the removal of nitrogen and phosphorus compounds, whereas organisms of activated sludge for biodegradation of organic compounds [40]. This mechanism may be especially important in wastewater treatment systems [41]. Traditional WWTPs based on activated sludge require costly technological solutions for the complex removal of biogenes [42]. Aerobic-anaerobic conditions must be ensured to enable the sequence of ammonification, nitrification, denitrification, and release processes, followed by accumulation of orthophosphates [43]. These are technologically complicated solutions requiring vast financial outputs for aeration and an advanced circulation system inside the installation [44]. The microalgae of the M-BGS structure are also responsible for the production of oxygen indispensable for bacteria [13]. Decreasing oxygen demand is the major obstacle in reducing energy consumption and emission levels of wastewater treatment systems based on the activated sludge method. Oxygen produced by microalgae has been proved to aid the metabolism of bacteria and improve technological and economic effectiveness [45]. On the other hand, bacterial biodegradation of pollutants results in the formation of mineralization forms of nitrogen and phosphorus, and carbon dioxide, which intensify microalgae development in M-BGS structure [46]. Van Nguyen et al. (2021) [47] proved that treatment efficiency of synthetic wastewater in the M-BGS system reached 96.5% for COD, 78–85% for nitrogen compounds, and 80.8% for phosphorus compounds [47]. In turn, the M-BGS system analyzed by Wang et al. (2021) [32] ensured 98% efficiency of COD removal from synthetic wastewater and removal efficiencies of biogenes at 78% for nitrogen compounds and 71% for phosphorus compounds [32]. It has also been proved that increased concentrations of biodegradable organic compounds in the environment modify the microalgae metabolism pattern into mixotrophic or even heterotrophic, which enhances the removal of carbon substances from wastewater [48,49].

3.2. Stage 2—M-BGS Anaerobic Digestion

Nominal biogas production from the pure *Chlorella* sp. culture was 440 ± 16 cm^3/gVS (Figure 15). CH_4 fraction was around 57.2 ± 1.4% (Table 6). The results indicate that higher abundance of activated sludge microbes in the M-BGS leads to better anaerobic digestion performance (Figure 15). Anaerobic digestion of the 15-day biomass produced 451 ± 22 cm^3/gVS biogas containing 60.2 ± 2.1% CH_4 (Table 6).

Table 6. Indicators of hydrophyte biomass AD performance.

Indicator		Unit	Phase of Experiment				
			Start	**15 Days**	**30 Days**	**45 Days**	**60 Days**
Biogas	Output	cm^3/gVS	440 ± 16	451 ± 22	459 ± 29	531 ± 36	506 ± 38
		cm^3/gTS	501 ± 18	530 ± 26	546 ± 34	661 ± 45	615 ± 46
	r rate	cm^3/gVS· d	57.2 ± 1.4	63.14 ± 2.6	59.7 ± 3.4	79.7 ± 5.1	75.9 ± 4.3
	Rate constant (k)	1/day	0.13 ± 0.01	0.14 ± 0.02	0.13 ± 0.02	0.15 ± 0.03	0.15 ± 0.03
Methane	Methane fraction	%	59.1 ± 2.0	60.2 ± 2.1	60.7 ± 3.1	66.2 ± 2.7	65.5 ± 3.0
	Output	cm^3/gVS	260 ± 9	271 ± 13	275 ± 15	350 ± 17	329 ± 20
		cm^3/gTS	295 ± 10	318 ± 15	327 ± 18	436 ± 21	400 ± 24
	r rate	cm^3/gVS· d	36.3 ± 0.8	37.9 ± 1.4	38.6 ± 1.8	52.5 ± 2.6	49.3 ± 2.4
	Rate constant (k)	1/day	0.14 ± 0.01	0.14 ± 0.02	0.14 ± 0.02	0.15 ± 0.03	0.15 ± 0.03

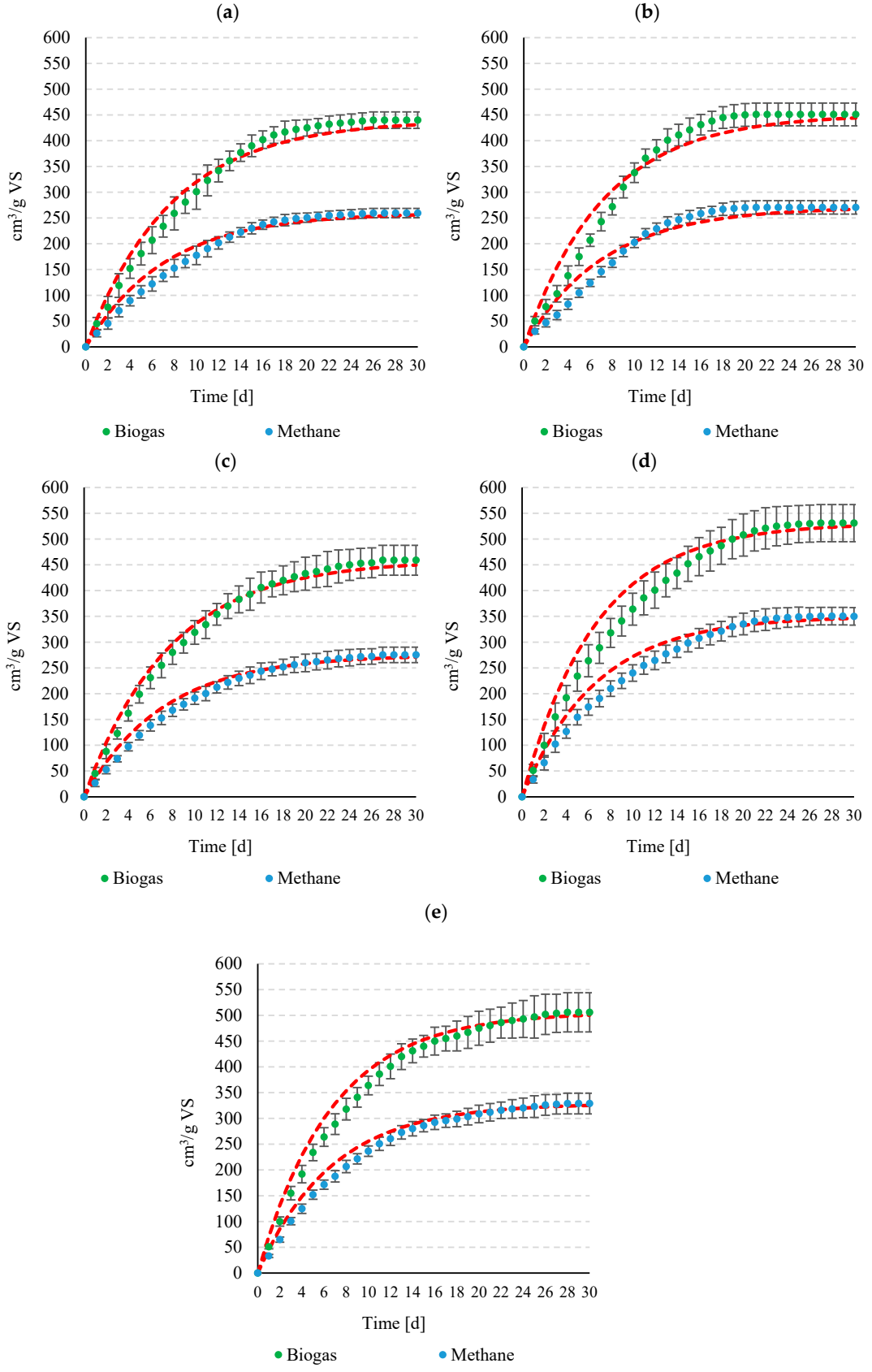

Figure 15. Trends in biogas and methane production in the anaerobic respirometers: (**a**) pure *Chlorella* sp. Culture; (**b**) biomass after 15 days' PBR operation; (**c**) biomass after 30 days' PBR operation; (**d**) biomass after 45 days' PBR operation; and (**e**) biomass after 60 days' PBR operation.

The M-BGS produced after 30 days of experiment was similar in terms of anaerobic digestibility. There were no statistically significant differences in gas output from fermentative bacteria. Biomass production was 459 ± 29 cm^3/gVS, containing 60.7 ± 3.1% CH_4 (Table 6). CH_4 output from the biomass in phases 1 (14 d) and 2 (30 d) of PBR operation was similar, at 271 ± 13 cm^3CH_4/gVS and 275 ± 15 cm^3CH_4/gVS, respectively (Figure 15).

On the other hand, significantly better performance was noted for anaerobic digestion of 45- and 60-day M-BGS. Biogas yields were 531 ± 36 cm^3/gVS from phase 3 biomass and 506 ± 38 cm^3/gVS from phase 4 biomass (Figure 15). The bacteria- and protozoa-rich biomass produced significantly higher rates of CH_4 in the biogas (over 65%). P3 and P4 showed the highest biogas production rates at 79.7 ± 5.1 cm^3/gVS·d and 75.9 ± 4.3 cm^3/gVS·d, respectively (Table 6). The C/N ratio, N levels, TOC, and biomass pH were found to very strongly correlate with AD performance (biogas/methane yields) (Figure 16).

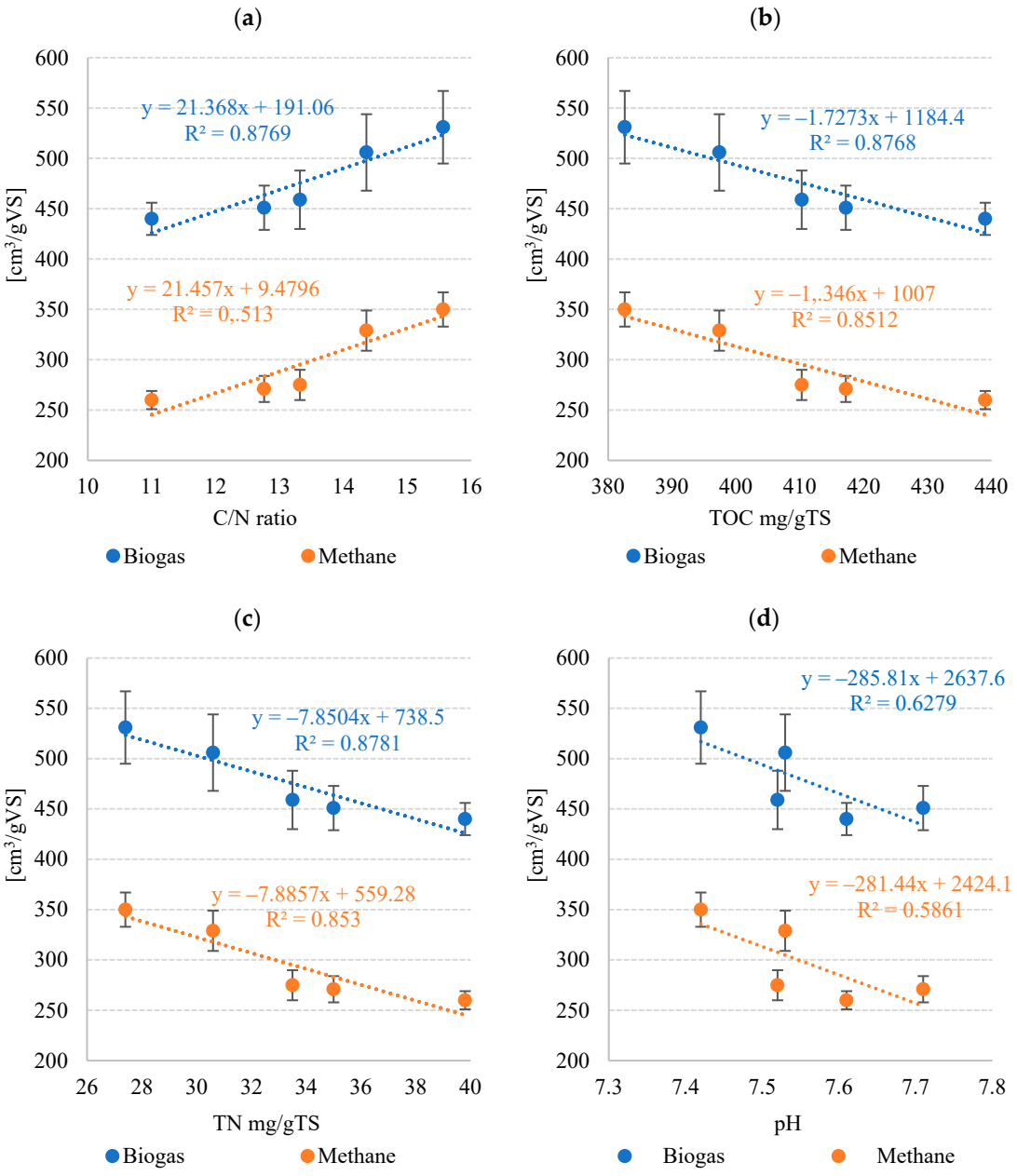

Figure 16. Correlations between selected biomass parameters (across growth phases) and biogas/methane yields: (**a**)—C/N ratio, (**b**)—TOC, (**c**)—TN, and (**d**)—pH.

There is a lack of reports in the available literature that would describe the effectiveness of M-BGS anaerobic digestion. For this reason, the results achieved in this study were referred to the findings from experiments into co-digestion of microalgal biomass and sewage sludge [50,51]. Anaerobic digestion of microalgae (*Chlorella* mixture) and excess sewage sludge performed by Hidaka et al. (2017) [50] for 28 days under laboratory conditions allowed the production of approximately 0.26 ± 0.02 dm^3CH_4/gVS under standard conditions of 101.3 kPa and 273.15 K [50]. Beltrán et al. (2016) [52] optimized the process of methane co-digestion of *Chlorella sorokiniana* and wastewater activated sludge (WAS) by testing various ratios of substrates (0% WAS-100% microalgae; 25% WAS-75% microalgae; 50% WAS-50% microalgae; 75% WAS-25% microalgae; 100% WAS-0% microalgae). They obtained the highest methane yield, i.e., 442 cm^3CH_4/gVS, using the 75% WAS-25% microalgae mixture [52]. Different substrate ratios were established by Adewale (2014) [53], who investigated co-digestion of *Chlorella vulgaris* and WAS. The results of their study demonstrated the linear correlation of the microalgae addition to WAS with methane yield until algae reaches a share of 75% in the co-digested mixture, when methane yield reached 369 cm^3CH_4/gVS. This finding formed grounds for developing a laboratory-scale CSTR in order to identify possible operational parameters and challenges likely to be encountered during continuous reactor work. The microalgae to WAS ratio of 75:25, OLR at 4 g $VS/dm^3 \cdot d$, and HRT of 20 days ensured the highest methane yield at 434 cm^3CH_4/gVS, suggesting a balance between the substrates, one which in turn promotes methanogenic activity [53]. Important issues to consider for the full-scale installation include ensuring stable work and optimal biogas production without compromising the post-fermentation characteristics of the residue. The composition of substrates is essential to a stable degradation process. A too low C/N ratio, as in the case of microalgal biomass, may lead to a high level of ammonia which inhibits biomethane production, especially at high process temperatures [54]. Further research is needed to identify optimal operation conditions (ratios, feeding rate, retention time), and to assess the impact of substrate characteristics on the methane fermentation of M-BGS.

4. Conclusions

Using M-BGS is still strictly in the realm of Research & Development, unlike purely bacterial aerobic and anaerobic granular sludge. Processes that mediate microalgae-bacterial granulation have not yet been fully understood. There is a dearth of research exploring how various operational and environmental parameters affect the process and how to maintain the granules for long-term bioreactor use. Therefore, there is a real need to obtain more data, especially with studies on scales of operation close to those of commercially-run plants.

The present study demonstrates that treatment of LF-DSS with *Chlorella* sp. can produce a growing microalgae + AS microbe community that can merge into M-BGS. The final stage of taxonomic and morphological evolution of the M-BGS was reached after 60 days' PBR operation. Afterwards, no further changes were noted in the morphology, taxonomic structure, chemical composition, LF-DSS treatment performance, and anaerobic digestibility of the M-BGS biomass. The biomass was abundant not only in *Chlorella* sp. microalgae, but also in filamentous *Microthrix parvicella*, and type 1851 and 1701 filamentous bacteria. Unicellular and protozoan species were much slower to grow. Activated sludge microbes accounted for approx. 43%TS of the entire M-BGS community.

Bacteria population growth significantly affected population growth curves, while also increasing the M-BGS biomass growth rate and final concentration in the H-PBR. A significantly higher final biomass concentration was observed after 45 days of LF-DSS treatment.

The higher levels of M-BGS biomass and the grown abundance of heterotrophic microbes were the major factors in improving organic pollutant removal from the LF-DSS. On the other hand, no relationship was found between these M-BGS parameters and N/P removal. Nutrients were effectively taken up during all phases of H-PBR operation. Changes in taxonomic composition of the M-BGS affected the chemical characteristics of the biomass, as well as the biogas composition and yield. Higher abundance of bacteria in

the M-BGS improves the C/N ratio, which in turn leads to significantly higher anaerobic digestion performance.

Future research into M-BGS-based technologies should focus on further understanding of microalgae-bacteria interactions. Data on these mechanisms, supported by reliable and comprehensive research, is necessary to develop technical and technological guidelines for biodegradation and pollutant removal, which can be implemented on a large scale. In-depth knowledge will also allow for the development of optimization procedures and empirical equations enabling the prediction of possible technological effects, including the efficiency of biomass growth, its biochemical composition, the efficiency of pollutant removal and the production of energy carriers or other value-added products. There have been no studies conducted on a pilot scale or in conditions close to real, which limits the possibility of reliable estimation of investment and operating costs of technologies based on M-BGS. The results of experimental work on a larger scale are also necessary to conduct a life cycle analysis (LCA), which in the longer term will allow the verification of the extension of the M-BGS application in other areas, such as bioenergy (e.g., methane, biohydrogen, biodiesel, or bioelectricity) and production biochemicals (e.g., polyhydroxyalkanoates or exopolysaccharides) at reduced process costs.

Author Contributions: Conceptualization, J.K.; Methodology, J.K. and M.D.; Validation, J.K.; Formal analysis, J.K.; Investigation, J.K.; Resources, J.K., M.D. and M.Z.; Software, J.K.; Data curation, J.K., M.D. and M.Z.; Writing—original draft preparation, J.K. and M.D.; Writing—review and editing, J.K., M.D. and M.Z.; Visualization, J.K. and M.D.; Funding acquisition, J.K. All authors have read and agreed to the published version of the manuscript.

Funding: The manuscript was supported by Project financially supported by Minister of Education and Science in the range of the program entitled "Regional Initiative of Excellence" for the years 2019–2023, project no. 010/RID/2018/19, amount of funding: 12,000,000 PLN, and the work WZ/WB-IIŚ/3/2022, funded by the Minister of Education and Science.

Institutional Review Board Statement: Not applicable.

Informed Consent Statement: Not applicable.

Data Availability Statement: Not applicable.

Conflicts of Interest: The authors declare no conflict of interest.

References

1. Jóźwiakowski, K.; Bugajski, P.; Kurek, K.; de Fátima Nunes de Carvalho, M.; Almeida, M.A.A.; Siwiec, T.; Borowski, G.; Czekała, W.; Dach, J.; Gajewska, M. The Efficiency and Technological Reliability of Biogenic Compounds Removal during Long-Term Operation of a One-Stage Subsurface Horizontal Flow Constructed Wetland. *Sep. Purif. Technol.* **2018**, *202*, 216–226. [CrossRef]
2. Nihemaiti, M.; Miklos, D.B.; Hübner, U.; Linden, K.G.; Drewes, J.E.; Croué, J.P. Removal of Trace Organic Chemicals in Wastewater Effluent by UV/H2O2 and UV/PDS. *Water Res.* **2018**, *145*, 487–497. [CrossRef] [PubMed]
3. Xu, L.; Wu, C.; Liu, P.; Bai, X.; Du, X.; Jin, P.; Yang, L.; Jin, X.; Shi, X.; Wang, Y. Peroxymonosulfate Activation by Nitrogen-Doped Biochar from Sawdust for the Efficient Degradation of Organic Pollutants. *Chem. Eng. J.* **2020**, *387*, 124065. [CrossRef]
4. Guven, H.; Dereli, R.K.; Ozgun, H.; Ersahin, M.E.; Ozturk, I. Towards Sustainable and Energy Efficient Municipal Wastewater Treatment by Up-Concentration of Organics. *Prog. Energy Combust. Sci.* **2019**, *70*, 145–168. [CrossRef]
5. Zhang, J.; Qin, Q.; Li, G.; Tseng, C.H. Sustainable Municipal Waste Management Strategies through Life Cycle Assessment Method: A Review. *J. Environ. Manag.* **2021**, *287*, 112238. [CrossRef]
6. Dudek, M.; Dębowski, M.; Kazimierowicz, J.; Zieliński, M.; Quattrocelli, P.; Nowicka, A. The Cultivation of Biohydrogen-Producing Tetraselmis Subcordiformis Microalgae as the Third Stage of Dairy Wastewater Aerobic Treatment System. *Sustainability* **2022**, *14*, 12085. [CrossRef]
7. Smol, M.; Adam, C.; Preisner, M. Circular Economy Model Framework in the European Water and Wastewater Sector. *J. Mater. Cycles. Waste Manag.* **2020**, *22*, 682–697. [CrossRef]
8. Rani, S.; Ojha, C.S.P. Chlorella Sorokiniana for Integrated Wastewater Treatment, Biomass Accumulation and Value-Added Product Estimation under Varying Photoperiod Regimes: A Comparative Study. *J. Water Process. Eng.* **2021**, *39*, 101889. [CrossRef]
9. Sharma, R.; Mishra, A.; Pant, D.; Malaviya, P. Recent Advances in Microalgae-Based Remediation of Industrial and Non-Industrial Wastewaters with Simultaneous Recovery of Value-Added Products. *Bioresour. Technol.* **2022**, *344*, 126129. [CrossRef]
10. Jamshidi, S. Value-Added Innovation in Infrastructure Systems, Lessons Learned from Wastewater Treatment Plants. *TQM J.* **2019**, *31*, 1049–1063. [CrossRef]

11. Rene, E.R.; Ge, J.; Kumar, G.; Singh, R.P.; Varjani, S. Resource Recovery from Wastewater, Solid Waste, and Waste Gas: Engineering and Management Aspects. *Environ. Sci. Pollut. Res.* **2020**, *27*, 17435–17437. [CrossRef]
12. Wilén, B.M.; Liébana, R.; Persson, F.; Modin, O.; Hermansson, M. The Mechanisms of Granulation of Activated Sludge in Wastewater Treatment, Its Optimization, and Impact on Effluent Quality. *Appl. Microbiol. Biotechnol.* **2018**, *102*, 5005–5020. [CrossRef]
13. Ji, B. Towards Environment-Sustainable Wastewater Treatment and Reclamation by the Non-Aerated Microalgal-Bacterial Granular Sludge Process: Recent Advances and Future Directions. *Sci. Total. Environ.* **2022**, *806*, 150707. [CrossRef]
14. Tan, X.; Xie, G.J.; Nie, W.B.; Xing, D.F.; Liu, B.F.; Ding, J.; Ren, N.Q. High Value-Added Biomaterials Recovery from Granular Sludge Based Wastewater Treatment Process. *Resour. Conserv. Recycl.* **2021**, *169*, 105481. [CrossRef]
15. Chen, H.; Li, A.; Cui, D.; Cui, C.; Ma, F. Evolution of Microbial Community and Key Genera in the Formation and Stability of Aerobic Granular Sludge under a High Organic Loading Rate. *Bioresour. Technol. Rep.* **2019**, *7*, 100280. [CrossRef]
16. Kazimierowicz, J.; Dębowski, M. Aerobic Granular Sludge as a Substrate in Anaerobic Digestion—Current Status and Perspectives. *Sustainability* **2022**, *14*, 10904. [CrossRef]
17. Zhang, X.; Lei, Z.; Liu, Y. Microalgal-Bacterial Granular Sludge for Municipal Wastewater Treatment: From Concept to Practice. *Bioresour. Technol.* **2022**, *354*, 127201. [CrossRef]
18. Ji, B.; Shi, Y.; Yılmaz, M. Microalgal-Bacterial Granular Sludge Process for Sustainable Municipal Wastewater Treatment: Simple Organics versus Complex Organics. *J. Water Process. Eng.* **2022**, *46*, 102613. [CrossRef]
19. Sun, P.; Liu, C.; Li, A.; Ji, B. Using Carbon Dioxide-Added Microalgal-Bacterial Granular Sludge for Carbon-Neutral Municipal Wastewater Treatment under Outdoor Conditions: Performance, Granule Characteristics and Environmental Sustainability. *Sci. Total. Environ.* **2022**, *848*, 157657. [CrossRef]
20. Fan, S.; Ji, B.; Abu Hasan, H.; Fan, J.; Guo, S.; Wang, J.; Yuan, J. Microalgal–Bacterial Granular Sludge Process for Non-Aerated Aquaculture Wastewater Treatment. *Bioprocess. Biosyst. Eng.* **2021**, *44*, 1733–1739. [CrossRef]
21. Wang, S.; Zhu, L.; Ji, B.; Hou, H.; Ma, Y. Microalgal-Bacterial Granular Sludge Process in Non-Aerated Municipal Wastewater Treatment under Natural Day-Night Conditions: Performance and Microbial Community. *Water* **2021**, *13*, 1479. [CrossRef]
22. Zhang, Y.; Zha, M.; Gao, M.; Wang, X. How Weak Static Magnetic Field Contributes to Rapid Granulation and Better Performance of Microalgal-Bacterial Granular Sludge? *Chem. Eng. J.* **2022**, *450*, 138162. [CrossRef]
23. Cao, J.; Chen, F.; Fang, Z.; Gu, Y.; Wang, H.; Lu, J.; Bi, Y.; Wang, S.; Huang, W.; Meng, F. Effect of Filamentous Algae in a Microalgal-Bacterial Granular Sludge System Treating Saline Wastewater: Assessing Stability, Lipid Production and Nutrients Removal. *Bioresour. Technol.* **2022**, *354*, 127182. [CrossRef] [PubMed]
24. Jiang, Q.; Chen, H.; Fu, Z.; Fu, X.; Wang, J.; Liang, Y.; Yin, H.; Yang, J.; Jiang, J.; Yang, X.; et al. Current Progress, Challenges and Perspectives in the Microalgal-Bacterial Aerobic Granular Sludge Process: A Review. *Int. J. Environ. Res. Public. Health* **2022**, *19*, 13950. [CrossRef] [PubMed]
25. Ji, B.; Fan, S.; Liu, Y. A Continuous-Flow Non-Aerated Microalgal-Bacterial Granular Sludge Process for Aquaculture Wastewater Treatment under Natural Day-Night Conditions. *Bioresour. Technol.* **2022**, *350*, 126914. [CrossRef]
26. Corominas, L.; Byrne, D.M.; Guest, J.S.; Hospido, A.; Roux, P.; Shaw, A.; Short, M.D. The Application of Life Cycle Assessment (LCA) to Wastewater Treatment: A Best Practice Guide and Critical Review. *Water. Res.* **2020**, *184*, 116058. [CrossRef]
27. Aragón-Briceño, C.I.; Ross, A.B.; Camargo-Valero, M.A. Mass and Energy Integration Study of Hydrothermal Carbonization with Anaerobic Digestion of Sewage Sludge. *Renew. Energy* **2021**, *167*, 473–483. [CrossRef]
28. Zieliński, M.; Dębowski, M.; Kazimierowicz, J. The Effect of Static Magnetic Field on Methanogenesis in the Anaerobic Digestion of Municipal Sewage Sludge. *Energies* **2021**, *14*, 590. [CrossRef]
29. Dębowski, M.; Kazimierowicz, J.; Zieliński, M.; Bartkowska, I. Co-Fermentation of Microalgae Biomass and Miscanthus × Giganteus Silage—Assessment of the Substrate, Biogas Production and Digestate Characteristics. *Appl. Sci.* **2022**, *12*, 7291. [CrossRef]
30. Dębowski, M.; Zieliński, M.; Dudek, M.; Grala, A. Acquisition Feasibility and Methane Fermentation Effectiveness of Biomass of Microalgae Occurring in Eutrophicated Aquifers on the Example of the Vistula Lagoon. *Int. J. Green. Energy* **2014**, *13*, 395–407. [CrossRef]
31. Zhang, Y.; Dong, X.; Liu, S.; Lei, Z.; Shimizu, K.; Zhang, Z.; Adachi, Y.; Lee, D.J. Rapid Establishment and Stable Performance of a New Algal-Bacterial Granule System from Conventional Bacterial Aerobic Granular Sludge and Preliminary Analysis of Mechanisms Involved. *J. Water Process. Eng.* **2020**, *34*, 101073. [CrossRef]
32. Wang, J.; Lei, Z.; Tian, C.; Liu, S.; Wang, Q.; Shimizu, K.; Zhang, Z.; Adachi, Y.; Lee, D.J. Ionic Response of Algal-Bacterial Granular Sludge System during Biological Phosphorus Removal from Wastewater. *Chemosphere* **2021**, *264*, 128534. [CrossRef] [PubMed]
33. Dong, X.; Zhao, Z.; Yang, X.; Lei, Z.; Shimizu, K.; Zhang, Z.; Lee, D.J. Response and Recovery of Mature Algal-Bacterial Aerobic Granular Sludge to Sudden Salinity Disturbance in Influent Wastewater: Granule Characteristics and Nutrients Removal/Accumulation. *Bioresour. Technol.* **2021**, *321*, 124492. [CrossRef] [PubMed]
34. Wu, X.; Li, H.; Lei, L.; Ren, J.; Li, W.; Liu, Y. Tolerance to Short-Term Saline Shocks by Aerobic Granular Sludge. *Chemosphere* **2020**, *243*, 125370. [CrossRef]
35. Lyu, W.; Zhang, S.; Xie, Y.; Chen, R.; Hu, X.; Wang, B.; Guo, W.; Wang, H.; Xing, J.; Zhou, D. Effects of the Exogenous N-Acylhomoserine Lactones on the Performances of Microalgal-Bacterial Granular Consortia. *Environ. Pollut. Bioavailab.* **2022**, *34*, 407–418. [CrossRef]

36. Liu, L.; Xin, Y.; Tong, Z.H.; Zheng, Y.M.; Xie, J.F.; Zhao, Q.B.; Yu, H.Q. Storage Strategy of Aerobic Algae-Bacteria Granular Consortia in Photo-Sequencing Batch Reactor. *J. Clean. Prod.* **2022**, *363*, 132410. [CrossRef]
37. He, Q.; Chen, L.; Zhang, S.; Chen, R.; Wang, H.; Zhang, W.; Song, J. Natural Sunlight Induced Rapid Formation of Water-Born Algal-Bacterial Granules in an Aerobic Bacterial Granular Photo-Sequencing Batch Reactor. *J. Hazard. Mater.* **2018**, *359*, 222–230. [CrossRef]
38. Shen, Y.; Zhu, L.; Ji, B.; Fan, S.; Xiao, Y.; Ma, Y. Reactivation of Frozen Stored Microalgal-Bacterial Granular Sludge under Aeration and Non-Aeration Conditions. *Water* **2021**, *13*, 1974. [CrossRef]
39. Fan, S.; Zhu, L.; Ji, B. Deciphering the Effect of Light Intensity on Microalgal-Bacterial Granular Sludge Process for Non-Aerated Municipal Wastewater Treatment. *Algal Res.* **2021**, *58*, 102437. [CrossRef]
40. Iqbal, K.; Saxena, A.; Pande, P.; Tiwari, A.; Chandra Joshi, N.; Varma, A.; Mishra, A. Microalgae-Bacterial Granular Consortium: Striding towards Sustainable Production of Biohydrogen Coupled with Wastewater Treatment. *Bioresour. Technol.* **2022**, *354*, 127203. [CrossRef]
41. Kant Bhatia, S.; Ahuja, V.; Chandel, N.; Mehariya, S.; Kumar, P.; Vinayak, V.; Saratale, G.D.; Raj, T.; Kim, S.H.; Yang, Y.H. An Overview on Microalgal-Bacterial Granular Consortia for Resource Recovery and Wastewater Treatment. *Bioresour. Technol.* **2022**, *351*, 127028. [CrossRef]
42. Rahimi, S.; Modin, O.; Mijakovic, I. Technologies for Biological Removal and Recovery of Nitrogen from Wastewater. *Biotechnol. Adv.* **2020**, *43*, 107570. [CrossRef]
43. Di Capua, F.; de Sario, S.; Ferraro, A.; Petrella, A.; Race, M.; Pirozzi, F.; Fratino, U.; Spasiano, D. Phosphorous Removal and Recovery from Urban Wastewater: Current Practices and New Directions. *Sci. Total. Environ.* **2022**, *823*, 153750. [CrossRef]
44. Petta, L.; De Gisi, S.; Casella, P.; Farina, R.; Notarnicola, M. Evaluation of the Treatability of a Winery Distillery (Vinasse) Wastewater by UASB, Anoxic-Aerobic UF-MBR and Chemical Precipitation/Adsorption. *J. Environ. Manag.* **2017**, *201*, 177–189. [CrossRef]
45. Ji, B.; Liu, Y. Assessment of Microalgal-Bacterial Granular Sludge Process for Environmentally Sustainable Municipal Wastewater Treatment. *ACS ES&T. Water* **2021**, *1*, 2459–2469. [CrossRef]
46. Hou, H.; Wang, S.; Ji, B.; Zhang, Y.; Pi, K.; Shi, Y. Adaptation Responses of Microalgal-Bacterial Granular Sludge to Polystyrene Microplastic Particles in Municipal Wastewater. *Environ. Sci. Pollut. Res.* **2022**, *29*, 59965–59973. [CrossRef]
47. Van Nguyen, B.; Yang, X.; Hirayama, S.; Wang, J.; Zhao, Z.; Lei, Z.; Shimizu, K.; Zhang, Z.; Le, S.X. Effect of Salinity on Cr(VI) Bioremediation by Algal-Bacterial Aerobic Granular Sludge Treating Synthetic Wastewater. *Process* **2021**, *9*, 1400. [CrossRef]
48. Chalima, A.; Oliver, L.; De Castro, L.F.; Karnaouri, A.; Dietrich, T.; Topakas, E. Utilization of Volatile Fatty Acids from Microalgae for the Production of High Added Value Compounds. *Ferment* **2017**, *3*, 54. [CrossRef]
49. Choi, W.J.; Chae, A.N.; Song, K.G.; Park, J.; Lee, B.C. Effect of Trophic Conditions on Microalga Growth, Nutrient Removal, Algal Organic Matter, and Energy Storage Products in Scenedesmus (Acutodesmus) Obliquus KGE-17 Cultivation. *Bioprocess. Biosyst. Eng.* **2019**, *42*, 1225–1234. [CrossRef]
50. Hidaka, T.; Takabe, Y.; Tsumori, J.; Minamiyama, M. Characterization of Microalgae Cultivated in Continuous Operation Combined with Anaerobic Co-Digestion of Sewage Sludge and Microalgae. *Biomass. Bioenergy* **2017**, *99*, 139–146. [CrossRef]
51. Kim, J.; Kang, C.M. Increased Anaerobic Production of Methane by Co-Digestion of Sludge with Microalgal Biomass and Food Waste Leachate. *Bioresour. Technol.* **2015**, *189*, 409–412. [CrossRef] [PubMed]
52. Beltrán, C.; Jeison, D.; Fermoso, F.G.; Borja, R. Batch Anaerobic Co-Digestion of Waste Activated Sludge and Microalgae (Chlorella Sorokiniana) at Mesophilic Temperature. *J. Environ. Sci. Health Part A* **2016**, *51*, 847–850. [CrossRef] [PubMed]
53. Adewale, O.A. Enhancing Methane Production in the UK WWTP Via Co-Digestion of Microalgae and Sewage Sludge. Ph.D. Dissertation, University of Leeds, Leeds, UK, 2014.
54. Thorin, E.; Olsson, J.; Schwede, S.; Nehrenheim, E. Co-Digestion of Sewage Sludge and Microalgae—Biogas Production Investigations. *Appl. Energy* **2018**, *227*, 64–72. [CrossRef]